SPH SIMULATION OF WATER WAVES GENERATED BY GRANULAR LANDSLIDES

Stefano Falappi[(1)], Mario Gallati[(2)]

[(1)]Hydraulic and Environmental Eng. Dept. (HEED), University of Pavia, 1 Via Ferrata, 27100 Pavia, Italy, phone: +39 0382 985323; fax: +39 0382 985589; e-mail: falappi@unipv.it

[(2)]Hydraulic and Environmental Eng. Dept. (HEED), University of Pavia, 1 Via Ferrata, 27100 Pavia, Italy, phone: +39 0382 985331; fax: +39 0382 985589; e-mail: gallati@unipv.it

ABSTRACT

The paper refers on SPH simulations of an experimental test concerning the impact of a granular landslide in a reservoir. In order to capture this phenomenon a model suitable for the treatment of granular material is implemented.

The experimental data are then compared to the results of the numerical simulation and discussed in detail to focus the capacities and the limits of the model.

Keywords: numerical model, SPH, granular material, water waves.

1 INTRODUCTION

This paper describes some results of the activities carried out at the Hydraulic and Environmental Eng. Dept. (HEED) of Pavia University in cooperation with CESI and CESI RICERCA. The activities concern the development of numerical models suitable for the simulation of landslides impact in a reservoir and the related hydrodynamics. Here we present the simulation of an experiment selected as a validation test case of the developed code.

The impact of a landslide in a reservoir is a phenomenon strictly related to the safety of the regions close to the basin. This event may cause strong effects as the formation of large water waves in the reservoir, the wave run up on the slope of the basin, the flooding of built-up areas and the dam overflowing or the dam breaking.

In Italy, due to well known disasters (e.g. Pontesei 1959; Vajont 1963), the reservoirs under risk are now kept largely “empty” to reduce the effect of a possible disaster, with heavy losses in energy production. Numerical tools, suitable for the realistic simulation of the relevant characteristics of the wave consequent to the falling of a landslide, could be useful in evaluating the filling level of the reservoir both safe and useful for the exploitation.

Such numerical models must be able to deal with the typical features of the considered phenomenon as unsteady free surfaces and interfaces, non hydrostatic pressure distribution; moreover they must be able to simulate the different rheological behaviour of the landslides from non deformable body to non-Newtonian mud or granular debris flow.

Our previous experience (Gallati & Braschi, 2000) leaded us to investigate the possibility of working with the SPH Lagrangian method, applied with good results in hydrodynamics. The method has proved useful in simulation of experimental tests concerning impacts of rigid bodies and Newtonian mud in a reservoir (Gallati & Braschi, 2003; Gallati et al., 2005; Gallati et al., 2006).

In this paper the SPH technique is employed to reproduce the hydrodynamics due to the impact of a granular landslide in a reservoir. In particular we focus on a experimental test carried out by Fritz and Hager (Fritz, 2002; Fritz et al., 2004) at ETH in Zurich. The experiment concerns the discharge of a dry granular material in a rectangular channel.

After a short review of the interpolation technique, we present the main features of the models implemented in the code and the numerical results of the simulation.

2 NUMERICAL MODEL

The model is bidimensional in the vertical plane. It is based on the Lagrangian SPH (Smoothed Particle Hydrodynamics) technique, first developed for astrophysical problems (Lucy, 1977; Monaghan & Gingold, 1977) and later employed in hydrodynamics. The technique is particularly suitable for the simulation of unsteady flows with free surfaces and interfaces (Monaghan, 1994; Monaghan et al., 1999).

In the view of the SPH technique a material continuum is seen as a distribution of interacting fictitious particles having mass m and bringing information in term of density, velocity, pressure, etc. Mass and the related flow quantities are distributed around the particle centroid according to a kernel function $W(\mathbf{x}, h)$ of unit volume and finite support $2h$.

In each point i, identified by the vector position $\mathbf{x}_i$, the value of a flow quantity and its derivatives are recovered summing up the contributions of the particles belonging to the circular region with radius $2h$, centred at the point i, by suitable interpolar expressions.

Using such interpolar expressions the continuous flow equations in Lagrangian form are discretized for each particle and explicitly solved for the time interval δt to get the flow characteristics (velocity, density, etc.) of each particle at the advanced time step starting from an initial distribution.

2.1 REVIEW OF THE INTERPOLATION TECHNIQUE

In the vertical plane (x, z) the value of a scalar function A, defined over a continuum material Ω of density ρ, could be written as:

$$A(\mathbf{x}) = \int_{\Omega} \delta(\mathbf{x} - \mathbf{x}')\, A(\mathbf{x}')\, d\mathbf{x}' \tag{1}$$

where $\mathbf{x} = (x, z)$ is the vector position and δ is the Dirac function.

In eq. (1) the Dirac function could be replaced by a kernel function $W(\mathbf{x}, h)$ of unit volume and finite support $2h$:

$$A(\mathbf{x}) = \int_{\Omega} W(\mathbf{x} - \mathbf{x}', h)\, A(\mathbf{x}')\, d\mathbf{x}' \tag{2}$$

The kernel function adopted in this work is the classical 3rd order spline (Monaghan, 1994):

$$W(\mathbf{x} - \mathbf{x}', h) = \frac{5}{14\pi} \frac{1}{h^2} \begin{cases} (2-q)^3 - 4(1-q)^3 & 0 \le q < 1 \\ (2-q)^3 & 1 \le q < 2 \\ 0 & q \ge 2 \end{cases} \tag{3}$$

where $q = \dfrac{|\mathbf{x} - \mathbf{x}'|}{h}$.

When, in the view of the SPH technique, the material continuum Ω is seen as a distribution of interacting particles having mass m_j and bringing flow quantities, then the value of the variable A is evaluated by eq. (2) in the discrete form:

$$\langle A(\mathbf{x}) \rangle = \sum_j \frac{m_j}{\rho_j} A(\mathbf{x}_j)\, W(\mathbf{x} - \mathbf{x}_j, h) \tag{4}$$

where m_j and ρ_j are the j-particle mass and density and the ratio m_j/ρ_j replaces the integration element $d\mathbf{x}'$.

Similarly, spatial derivatives of the variable A are evaluated by an interpolating summation involving the derivatives of the kernel function. As example the gradient of the

variable A is:

$$\langle \nabla A(\mathbf{x}) \rangle = \sum_j \frac{m_j}{\rho_j} A(\mathbf{x}_j) \nabla W(\mathbf{x} - \mathbf{x}_j, h) \tag{5}$$

Actually modified expression, not quoted here, are used to numerically account the action-reaction principle between particles (Monaghan, 1994).

2.2 NUMERICAL MODEL FOR NEWTONIAN FLUID

The Newtonian fluid is modelled as slightly compressible in isothermal conditions, thus the pressure p is related to the density ρ through the sound speed c with the state equation:

$$p = c^2(\rho - \rho_0) \tag{6}$$

got by suitable first order approximation of the full equation around the reference state $\rho=\rho_0$, $p=0$.

The continuity and the motion constraints are stated in Lagrangian form by:

$$\frac{D\rho}{Dt} = -\rho \nabla \cdot \mathbf{v} \tag{7}$$

$$\frac{D\mathbf{v}}{Dt} = -\frac{1}{\rho}\nabla p + \frac{1}{\rho}\nabla \cdot \boldsymbol{\tau} + \mathbf{g} \tag{8}$$

where $\mathbf{v}$ is the velocity, $\mathbf{g}$ is the gravity acceleration. The shear stress tensor $\boldsymbol{\tau}$ for a Newtonian fluid is related to the rate of deformation tensor $\mathbf{S}$ by the dynamic viscosity μ of the fluid:

$$\boldsymbol{\tau} = 2\mu \mathbf{S} \tag{9}$$

Substituting eq. (9) in eq. (8) we get:

$$\frac{D\mathbf{v}}{Dt} = -\frac{1}{\rho}\nabla p + \frac{1}{\rho}(\nabla \cdot \mu \nabla)\mathbf{v} + \mathbf{g} \tag{10}$$

The numerical counterparts of the Navier-Stokes equations (7,10), suitably designed to fulfil the action-reaction principle, are:

$$\frac{D\rho_i}{Dt} = \sum_j m_j (\mathbf{v}_i - \mathbf{v}_j) \cdot \nabla W_{ij} \tag{11}$$

$$\frac{D\mathbf{v}_i}{Dt} = -\sum_j m_j \frac{p_j - p_j}{\rho_i \rho_j} \nabla W_{ij} + \sum_j \frac{m_j(\mu_i + \mu_j)}{\rho_i \rho_j} \frac{\mathbf{v}_{ij}}{r_{ij}} \frac{\partial W_{ij}}{\partial r} + \mathbf{g} \tag{12}$$

where $r_{ij} = \mathbf{x}_i - \mathbf{x}_j$, $\mathbf{v}_{ij} = \mathbf{v}_i - \mathbf{v}_j$, $W_{ij} = W(r_{ij}, h)$.

In eq. (12) the viscous term is interpolated according to the Morris formulation (Morris et al. 1997).

2.3 NUMERICAL MODEL FOR GRANULAR MATERIAL

The granular material motion can be classified in different flow types according to the prevalent interaction between grains. Two main flow regimes can be identified: in the first one (frictional or slow flow) the particles concentration during motion is close to the concentration at rest and the friction is responsible of the main interaction between grains. In the second regime (collisional or rapid flow) the concentration of grains is lower than the maximum possible and the impact between grains is the main dissipative effect.

A large number of models have been used to describe the behaviour of granular material

during flow but in general, they model the granular material as a single-phase fluid with specific rheology to reproduce the main effects between grains.

In this work the granular material is simulated as a fluid with density ρ, equal to bulk density of the granular material. Moreover in the experiment taken into account the flow type is mainly frictional, and so we implement a proper rheological law that includes a Mohr-Coulomb yield criterion. This approach is suitable to reproduce the friction between grains and the stopping of the granular landslide and it has been implemented both in Eulerian (Frenette et al., 2002) and in Lagranian frame (Gutfraind and Savage, 1997; Rodriguez-Paz & Bonet, 2003; Shen et al., 2003).

Assuming that, during granular flow, the principal axes of the shear stress tensor match the principal axes of the rate of deformation tensor we can define the shear stress tensor as:

$$\boldsymbol{\tau} = 2\mu_{eff}\,\mathbf{S} \tag{13}$$

where μ_{eff} is the effective viscosity which is variable in each point of the granular material.

The effective viscosity is defined as:

$$\mu_{eff} = \frac{p\,sin\,\varphi}{\sqrt{4I_{2S}}} \tag{14}$$

where p is the pressure, φ is the internal friction angle and I_{2S} is the second invariant of the rate of deformation tensor.

In the view of SPH technique the single phase fluid simulating the granular material is seen as a distribution of particles. Eq. (11) and eq. (12) enable the description of the motion of these particles providing the definition of the effective viscosity (14) for each particle. It should be reminded that this requires the evaluation of the rate of deformation tensor and so the gradients of the velocity vector for each particle.

2.4 TIME INTEGRATION SCHEME

At beginning of the simulation the material continua are discretized by proper sets of particles using a proper spatial scale h. Position, mass, velocity, pressure and density are therefore fixed for each particle according to the initial state of the system and to the properties of the materials.

To reach the system configuration at following time steps we adopt an explicit 1st order staggered integration scheme in which the evaluation of the velocity is half time step staggered from the computational time of position, density and pressure.

The time step is controlled to satisfy the Courant condition and the constraint due to the viscous diffusion. The time step δt is related to the spatial scale h by the equation:

$$\delta t = \beta\, min\left\{\frac{h}{c + |\mathbf{v}_{max}|}, \frac{\rho h^2}{2\mu}\right\} \tag{15}$$

where β is a numerical coefficient and $\mathbf{v}_{max}$ is the maximum value of the velocity.

In order to increase the time step it is practical to take the value of the sound speed lower than the real one, but high enough so that the Mach number of the flow is lower than 0.1 (Monaghan, 1994; Morris et al., 1997). Thus the value of the sound speed must be chosen carefully to ensure an efficient and an accurate solution of the problem.

The effective viscosity in equation (14) attains an infinite value when I_{2S} tends to be infinitesimal. Such large value of viscosity will strictly reduce the time step and create numerical divergence. Thus the effective viscosity is numerically bounded by a fixed value μ_{max} to ensure convergence and a reasonable time step.

2.5 BOUNDARY CONDITIONS

In this work the solid walls are simulated using two different strategies: the effect of vertical and horizontal walls are represented via the classical mirror particle technique, while the fixed particles method is employed to model the solid boundaries having different slope.

The mirror particle technique requires the extension of the domain by a strip of thickness $2h$ in which the set of mirror particle is placed. For each particle in the domain, close to the borders less than $2h$, a mirror particle is created. The mirror particle is placed outside the domain reflecting the starting particle position through the borders. The mirror particle has the same density and pressure of the continuum particle, while the component of the velocity normal to the wall has the same modulus but opposite direction.

The second technique is suitable to model the solid boundaries with complex topography, that are not easily simulated via the mirror technique. In this approach a strip (thickness $2h$) of fixed particles is placed outside the wall boundary. These particles have only geometric quantities and their positions stay unchanged during the simulation. When the flow particle i interacts with a fixed particle, this last one takes the same mass, density and pressure of the flow particle, while the component of the velocity normal to the wall has the same modulus but opposite direction.

Different slip conditions could be applied along the boundaries. The choice of the slip boundary condition depends on the properties of the fluid, the geometrical shape of the boundaries, and the scale of particles.

For Newtonian fluid at low viscosity it is often possible to set a free slip condition on the wall boundaries avoiding the representation of the boundary layer. This condition in reached setting to the boundary particle (mirror or fixed) the same tangential velocity of the flow particle.

In the case of non-Newtonian fluids or granular materials the slip is mainly located near the wall and the simulation of the shear layer is necessary.

The physical no slip condition, reached setting to the boundary particle the opposite tangential velocity of the flow particle, requires a spatial scale of the particles small enough to accurately represent the velocity gradient in the shear layer. This could involve a great number of particles to discretize the material continuum and so an high computational cost. In such a situation it is applied a controlled slip condition setting the value of the tangential stress at the wall, computed via the laminar boundary layer approximation [Falappi, 2006].

3 MODEL VALIDATION

3.1 EXPERIMENT

The experiments are carried out at the Laboratory of Hydraulics, Hydrology and Glaciology (VAW) of the Swiss Institute of Technology (ETH) by Fritz and Hager (Fritz, 2002; Fritz et al., 2004). The test are performed in a 0.5 m thick rectangular channel schematized in Fig. 1. The horizontal length of the channel is 11 m. In Fig. 1 we represent only the length used in the simulation.

The landslides is simulated by a dry granular material. The grains are composed of a mixture of polypropylene and barium sulphate. The granulate properties are: grain density ρ_g=2640 kg/m^3, grain diameter d_g=4 mm, bulk slide porosity n=39%, bulk slide density ρ_s=1620 kg/m^3, effective internal friction angle φ =43° and dynamic bed friction angle δ=24°.

At the beginning of the experiment the granular material is stored in a box having the same width of the channel. The box is set in motion along the slope ramp by a pneumatic accelerator achieving high release velocity (V_s) of the granular material producing high impact velocity (V_i) of the landslide.

The still water level in the channel is h_w=0.3 m.

The impact Froude number is defined as below:

$$Fr = \frac{V_i}{\sqrt{gh_w}} \tag{16}$$

According to the authors observation the impact Froude number affects strongly both the water waves height and the water waves shape after impact. For low Froude number (Fr<2) there's no separation between granular material and water after impact. For higher values of the parameter (Fr>2) the large impact energy implies the separation between water and granular material and the formation of water crest that could collapse backward on the landslide (2<Fr<4) or outward on water in the channel (Fr>4).

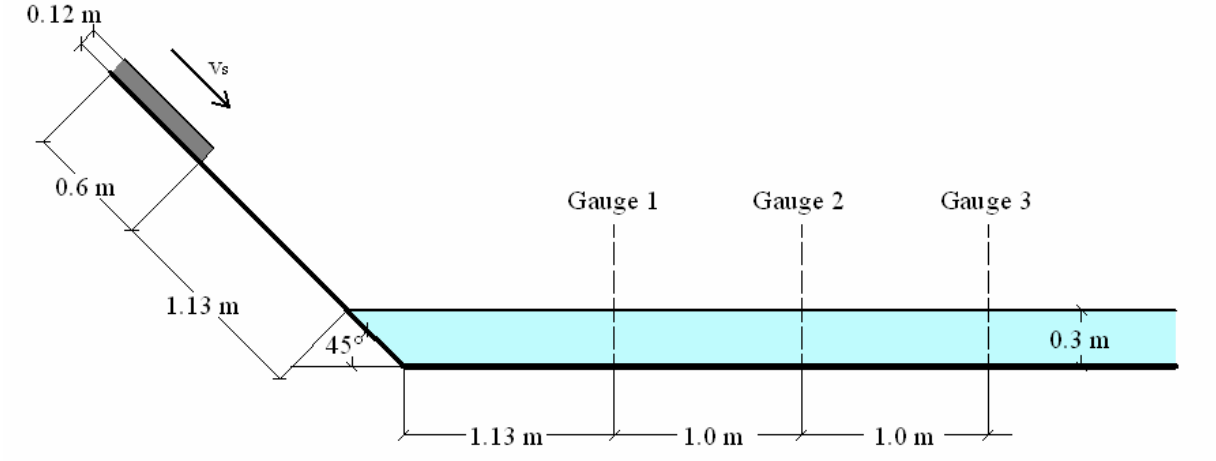

Figure 1. Geometric configuration of the experiment

The release velocity in the selected test is V_s=3.17 m/s, the centeroid impact velocity, evaluated by the authors, is V_i =4.8 m/s. The impact Froude number of this experiment is Fr=2.8.

The impact is recorded by digital camera and the water level fluctuations in the horizontal part of the channel are measured by capacitance wave gauges placed as in Fig. 1.

The main characteristics of the phenomenon are summarized in the pictures in the left column of Fig. 2. The impact instant is taken as the time origin.

The impact generates a large vertical water displacement that leads to the formation of a crest, while the granular material flows along the ramp (t=0.126 s). At time t=0.259 s the landslide reaches the channel bottom and the wave crest rises up to the local maximum level. The granular material slows down because of the absence of the driving force of the gravity, the backpressure of water and the dissipation between grains and between grains and the channel bottom (t=0.392 s). The upstream end of the crest falls on the ramp.

At t=0.527 s the kinetic energy of the landslide is completely dissipated and the changes in shape of the granular material are due to the interaction with the fluid above. The closure of the wave on the granular material entraps a large volume of air that strongly perturbs the water free surface and the flow near the ramp.

The water waves generated by the impact spread in the channel (t=0.660 s - t=0.793 s), while a part of the water volume of the crest rises up the ramp with strong splashes.

The granular material is dry at the beginning of the test. After impact water fills part of the granular interstitial pores discharging air. This phenomenon is almost absent just after impact (t=0.126 s – t=0.392 s), while it becomes very pronounced after the crest closure on the landslide (t=0.527 s – t=0.793 s). At these stages the interface between granular material and water isn't clear because of the rising up to the free surface of a large volume of air from

intergranular pores.

In Figure 3 the hydrographs recorded by the three gauges are presented.

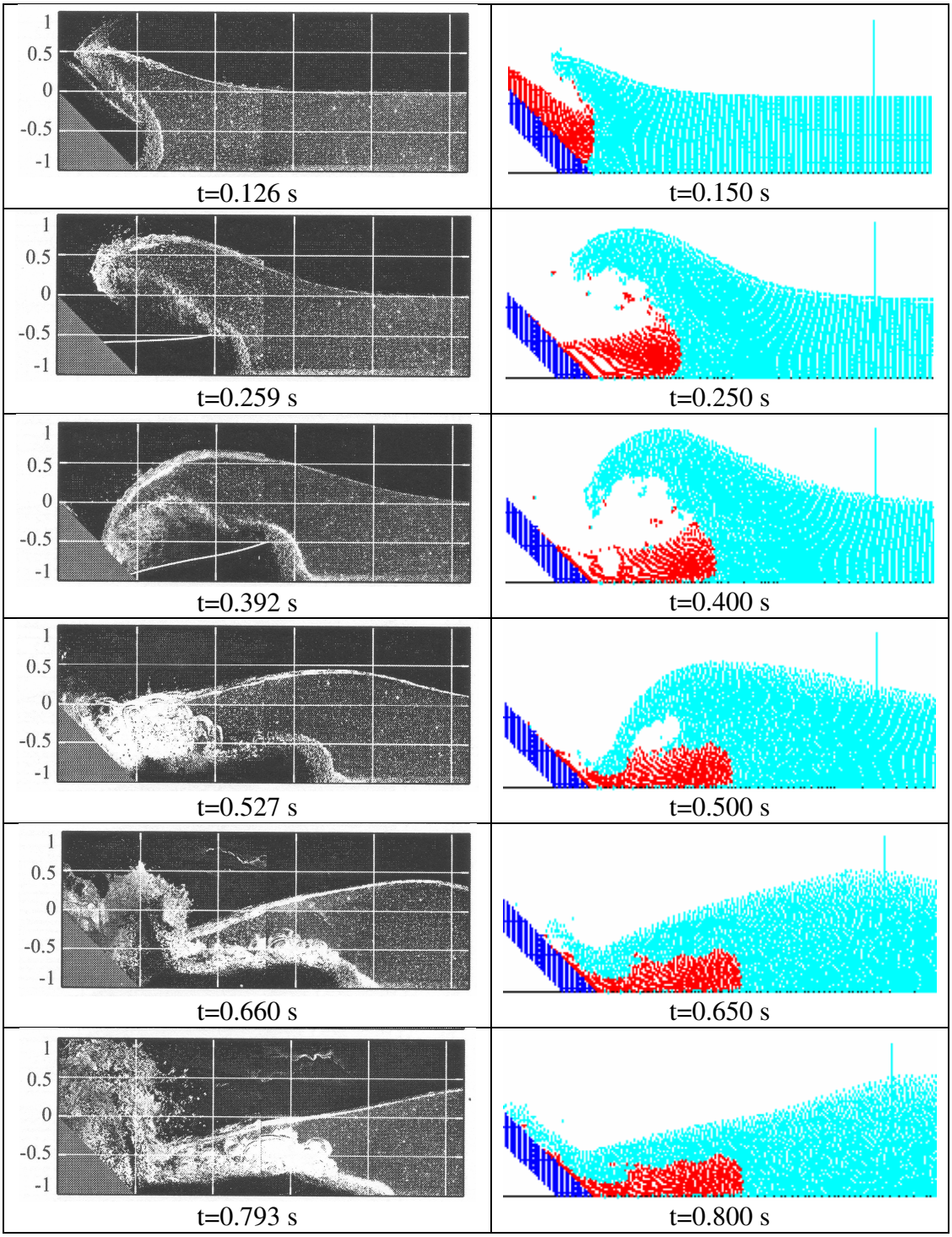

Figure 2. Experiment frame (left) and simulation picture (right).

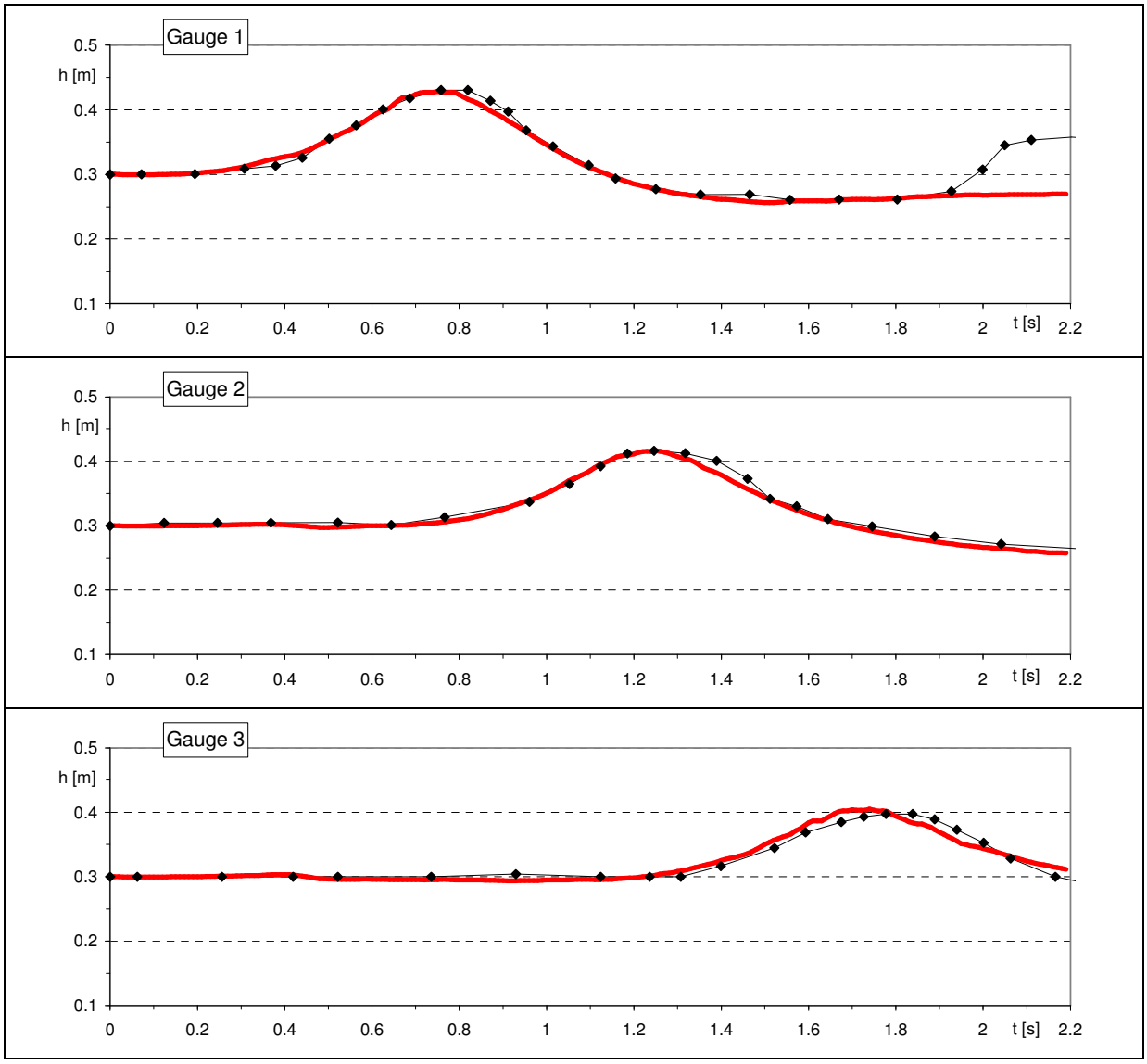

Figure 3. Hydrographs (black dots: experimental data, red line: numerical simulation).

3.2 SIMULATION

The length of the channel is reduced to 4.5 m. This approach allows to simulate of the experiment using a small enough particle scale otherwise the computational time becomes exceeding with the employed standard PC. Anyway the chosen channel length enables the simulation of the spreading of the first positive wave beyond the third gauge, but the simulated water levels at the gauges are meaningful only before the wave reflection from the downstream vertical wall.

The initial field is represented by a set of particles placed according to a regular grid with a step equal to 0.01 m. The total number of particles is close to 16000. The kernel scale h=0.015 m is adopted.

At the beginning of the simulation the particles representing the granular material assume a velocity equal to the release velocity (V_s=3.17 m/s), density equal to the bulk density of the granular material (ρ_s=1620 kg^3/m^3)and hydrostatic pressure distribution. The water particles have hydrostatic pressure and velocity equal to zero.

The time step (15) is evaluated using the following parameter: sound speed c=30 m/s, maximum effective viscosity μ_{max}=5000 Pa s and numerical coefficient β=0.4.

As quoted above, the effect of the horizontal bottom of the channel and of the downstream vertical wall is simulated via the mirror particle technique, while the ramp is represented by a set of fixed particles. On the solid boundaries the slip condition is imposed setting the value of the wall tangential stress.

In right column of Fig. 2 the numerical simulation pictures are compared with the corresponding experimental frames.

The simulation reproduces the main flow characteristics at the first stages of the phenomenon. In particular the vertical water displacement and the crest formation after impact are very similar to the experimental ones (t=0.150 s). The landslide propagation on the channel bottom and the rising up of the crest agree with the experiment (t=0.250 s).

At time t=0.400 s even if the landslide shape is close to the experimental one, the level reached by the wave crest is somewhat overvalued. Moreover in the simulation the crest falls on the granular material and not on the ramp as in the experiment (t=0.500 s).

It should be reminded that even if the experimental phenomenon is manly bidimensional the crest formation has strong tridimensional characteristics that cannot be captured by the simulation, strictly based on a 2D schematization.

The numerical simulation appreciably differs from the experiment after the crest impact on the granular landslide (t=0.650 s): the effect of the air volume entrapped by water is not represented and the free surface appears smooth. Moreover the simulation doesn't model the granular pores saturation and the subsequent air ejection (t=0.800 s).

In any case as the air entrapment and the tridimensional effects are damped moving downstream, the free surface shape is similar to the experimental one.

This is corroborated by the hydrographs in Fig. 3. In all the measuring gauges the simulated level fluctuations agree with the experimental measures: not only the maximum level reached by the wave and the water volume displaced, but also the characteristic times of the phenomenon agree with the experimental ones. It should be reminded that the characteristics of the water wave generated by the impact of a mass in a reservoir are deeply connected to the shape of the landslide and its impact kinetic energy. The fact that the main characteristics of the wave are well reproduced displays the simulation effectiveness and supports the proposed models and the adopted simplifications.

4 CONCLUSION

According to the results above presented the SPH technique is suitable to simulate the flow generated by the impact of a granular landslide in a reservoir.

In the considered situation the results are in reasonable agreement with the laboratory data, in particular the simulation reproduced the more relevant engineering quantities as the peak value of the wave, the displaced water volume and the characteristic times of the phenomenon.

We think that in the future the quality of the simulation results could be increased improving the granular material model, taking into account the effect of the dilatancy during flow and the intergranular pores saturation.

The simulation of a realistic phenomenon is the next target of the research. This requires a tridimensional version of the code. In this case the main difficulties are not related to the 3D extension of the model but to the management of the large number of particles needed to have 3D consistent simulations. As a matter of fact such a simulation implies the parallelization of the code and the use of parallel super calculator.

REFERENCES

Gallati, M., Braschi, G. (2000), Simulazione Lagrangiana di flussi con superficie libera in problemi di idraulica, *L'Acqua*, 5, pp.7–18.

Gallati, M., Braschi, G. (2003), SPH simulation of the wave produced by a block falling into a water tank, in *Proc. Int. Conf. on Fluid Flow Technologies (CMFF'03)*, Budapest.

Gallati, M., Braschi, G., Falappi, S. (2005), SPH simulations of the waves produced by a block falling into a reservoir, *Il Nuovo Cimento*, 28 C (2), pp.129–140.

Gallati, M., Braschi, G., Falappi, S. (2006), Esperienze di validazione sull'impatto di una massa fluida in un bacino, in *Atti del XXX Convegno di Idraulica e Costruzioni Idrauliche*, Roma.

Fritz, H.M. (2002), Initial phase of landslide generated impulse waves (PhD Thesis), VAW ETH ,Zurich.

Fritz, H.M., Hager, W.H., Minor, H.E. (2004), Near field characteristics of landslides generated impulse waves, *J. Waterway, Port, Coastal, and Ocean Eng.*, 130, pp.287–302.

Lucy, L.B. (1977), A numerical approach to the testing of the fission hypotesis, *Astron. Journ.*, 82, pp.1013–1020.

Monaghan, J.J., Gingold, R.A. (1977), Smoothed particle hydrodynamics: theory and application to non-spherical stars, *Mon. Not. R. Astr. Soc.*, 181, pp.375–389.

Monaghan, J.J. (1994), Simulating free surface flow with SPH, *Journ. of Comp. Physics*, 110, pp.399–406.

Monaghan, J.J., Cas, R.A.F., Kos, A.M., Hallworth, M. (1999), Gravity currents descending a ramp in a stratified tank, *J. Fluid Mech.*, 379, pp.39–69.

Morris, J.P., Fox, P.J., Zhu, Y. (1997), Modelling low Reynolds number incompressible flows using SPH, *Journ. of Comp. Physics*, 136, pp.214–226.

Frenette, R., Zimmermann, T., Eyheramendy, D. (2002), Unified modelling of fluid or granular flows on dam-break case, *J. Hydraulic Eng.*, 128, pp.299-305.

Gutfraind, R., Savage, S.B. (1997), Smoothed particle hydrodynamics for the simulation of broken-ice fields, *J. Comp. Phys.*, 134, pp.203-215.

Rodriquez-Paz, M.X., Bonet, J. (2003), A corrected smoothed particle hydrodynamics method for the simulation of debris flow, *Numer. Methods Partial Differential Eq.*, 20, pp.140-163.

Shao, S., Lo, E.Y.M. (2003), Incompressible SPH method for simulating Newtonian and non-Newtonian flows with a free surface, *Advances in Water Resources*, 26, pp.787-800.

Falappi, S. (2006), Simulazioni numeriche di flussi di fluidi viscosi e di materiali granulari con la tecnica SPH (PhD Thesis), HEED ,Università degli Studi di Pavia.